Wind Tunnel Results of the B-52B with the X-43A Stack

Mark C. Davis[*] and Alexander G. Sim[†]
NASA Dryden Flight Research Center, Edwards, California, 93523

Matthew Rhode[‡]
NASA Langley Research Center, Hampton, Virginia, 23681

and

Kevin D. Johnson[§]
AS&M, NASA Dryden Flight Research Center, Edwards, California, 93523

A low-speed wind-tunnel test was performed with a three-percent-scale model of a booster rocket mated to an X-43A research vehicle—a combination referred to as the Hyper-X launch vehicle. The test was conducted both in free-stream air and in the presence of a partial model of the B-52B airplane. The objectives of the test were to obtain force and moment data to generate structural loads affecting the pylon of the B-52B airplane and to determine the aerodynamic influence of the B-52B airplane on the Hyper-X launch vehicle to evaluate launch separation characteristics. The wind-tunnel test was conducted at a low-speed wind tunnel in Hampton, Virginia. All moments and forces reported are based either on the aerodynamic influence of the B-52B airplane or are for the Hyper-X launch vehicle in free-stream air. Overall, the test showed that the B-52B airplane imparts a strong downwash onto the Hyper-X launch vehicle, reducing the net lift of the Hyper-X launch vehicle. Also, pitching and rolling moments are imparted onto the booster and are a strong function of the launch–drop angle of attack.

Nomenclature

A	=	angle of attack polar
C_A	=	axial-force coefficient
C_D	=	drag coefficient
C_L	=	lift coefficient
C_l	=	rolling-moment coefficient
C_m	=	pitching-moment coefficient
C_N	=	normal-force coefficient
C_n	=	yawing-moment coefficient
C_Y	=	side-force coefficient
da	=	aileron position, deg [$da = de,r - de,l$]
de	=	elevator position, deg [$de = (de,r + de,l) / 2$]
de,l	=	left elevon fin position, deg
de,r	=	right elevon fin position, deg
dr	=	rudder fin position, deg

[*] Aerospace Engineer, Research Engineering, NASA Dryden Flight Research Center, P.O. Box 273, M/S 2228, Edwards, California, 93523, Senior AIAA member.

[†] Aerospace Engineer, Research Engineering, NASA Dryden Flight Research Center, P.O. Box 273, M/S 2228, Edwards, California, 93523, Senior AIAA member.

[‡] Aerospace Engineer, Research Engineering, NASA Langley Research Center, Hampton, Virginia, 23681, Senior AIAA member.

[§] Aerospace Engineer, AS&M, NASA Dryden Flight Research Center, P.O. Box 273, M/S 2228, Edwards, California, 93523, Senior AIAA member.

HXLV	=	Hyper-X launch vehicle		
HXRV	=	Hyper-X research vehicle		
LWD	=	left wing down		
ND	=	nose down		
MDOE	=	Modern Design of Experiments		
NL	=	nose left		
NR	=	nose right		
NU	=	nose up		
psf	=	pounds per square foot		
P-factor	=	proximity coefficient		
R	=	repeat		
RWD	=	right wing down		
RWU	=	right wing up		
RV	=	research vehicle		
α	=	angle of attack, deg		
β	=	angle of sideslip, deg		
Δ	=	incremental		

Configuration control combination definitions:

Configuration	*de*	*Dr*	*da*	Definition
0	0	0	0	Zero Controls
ND-NL	51	51	0	Nose down-nose left
ND-NR	51	–51	0	Nose down-nose right
NU-NL	–51	51	0	Nose up-nose left
NU-NR	–51	–51	0	Nose up-nose right
RWD-NL	0	–51	–102	Right wing down-nose left
RWU-NR	0	–51	102	Right wing up-nose right

Introduction

Three X-43A hypersonic research vehicles (RVs) were constructed for the purpose of conducting scramjet engine research. An alternate name for the X-43A vehicle was Hyper-X. Each vehicle was designed for one flight, and each was mounted on the front of a Pegasus® (Orbital Sciences Corporation, Chandler, Arizona) rocket booster in a configuration called the Hyper-X launch vehicle (HXLV) or the X-43A stack, which consisted of the Pegasus booster rocket, the Hyper-X research vehicle (HXRV), and the adapter. The HXLV was carried to the launch point by a modified B-52B airplane. Figure 1 shows the B-52B airplane carrying the HXLV stack. The captive carry of the X-43A was very similar to that of the X-15 rocket airplane (North American Aviation, Inglewood, California), which is detailed in reference 1. The flight test was performed in four phases. The first phase was the captive-carry phase, during which the B-52B airplane carried the X-43A stack to the launch point. The second phase was the drop-and-boost portion of the flight, during which the Pegasus booster rocket was dropped from the B-52B airplane and boosted the HXLV to the proper flight conditions. During the third phase, the boost was completed and the HXRV separated from the booster. The fourth and final phase, from the end of the separation through the test of the engine, ended when the HXRV splashed down into the ocean. This report focuses on the captive carry and initial launch separation of the HXLV from under the right wing of the B-52B airplane. Additional X-43A project information is detailed in reference 2.

The three large tail surfaces, or fins, on the HXLV were used as primary control effectors. For a nominal flight, 20 deg was the maximum fin deflection. The fins were powered by thermal batteries that had a life expectancy of approximately 10 min. Approximately 2 min prior to launch from the B-52B airplane, the batteries were powered up and the fin locking pins were retracted. A small-amplitude oscillation maneuver was then performed to ensure the proper operation of the fin system. Provided that all critical systems on both the booster rocket and the X-43A RV were operating properly, the HXLV would be launched. If a problem with any critical system was detected, the launch would be aborted, the fin pins reinserted, and the B-52B airplane would return to base with the HXLV. Reinserting the fin pins before battery exhaustion was an important element of this process because in subsonic

conditions the fins were statically unstable and would be driven to their 51-deg mechanical stop. This would result in an off-nominal condition and would only occur when there was no longer power to control the fins. Whereas the inability to reinsert the pins would only occur after multiple failures, the resulting structural loads into the B-52B airplane pylon were of concern.

The aerodynamics of the HXLV with full control surface deflections while in the influence of the B-52B airplane were not well understood, and it was not practical to even conservatively try to calculate the aerodynamic loads. These concerns precipitated the desire to conduct a wind-tunnel test to gather aerodynamic data of the HXLV in the proximity of the B-52B airplane. A transonic test including the fabrication of a partial B-52B airplane model would have been cost-prohibitive, and there was the possibility of tunnel blockage problems rendering the results inconclusive. Therefore, using an existing three-percent-scale HXLV model and fabricating a partial B-52B airplane model from plastic, tests were conducted in a low-speed wind tunnel in which blockage was less of a problem and the tests were accomplished relatively quickly. The resulting aerodynamic data would not be at the same conditions as that obtained from a transonic test but were considered conservative in the sense that the aerodynamic influences measured from a low-speed test were judged to be slightly greater than would be obtained from a test at transonic speeds. The ViGYAN Low-Speed Wind Tunnel (ViGYAN, Incorporated, Hampton, Virginia) with its open test section[3], was chosen for the test, which was conducted prior to the second X-43A flight.

The primary objective of the wind-tunnel test was to obtain a set of aerodynamic coefficients that could be used to calculate the structural pylon loads that result from a worst-case set of HXLV fin deflections. Thus, it was decided to conduct much of the wind-tunnel test with combinations of fin settings so that the coefficients could be directly applied to model the structural loads of the B-52B airplane pylon with the HXLV attached. An example set of these coefficients is shown in Figs. 7 through 14 of this report. As secondary objectives, limited sets of data were obtained with each fin deflected separately and with the HXLV in the wind tunnel without the B-52B airplane model (in free-stream flow). The free-stream data was used to show the increments associated with the HXLV being in the presence of the B-52B airplane. These increments were later used to derive a simplistic model for launch separation.

Wind Tunnel Description

The ViGYAN Low-Speed Wind Tunnel is an open-circuit facility with a rectangular open-jet test section 3 ft tall and 4 ft wide in cross-section and 5 ft long. The tunnel is powered by a variable-pitch, multi-blade fan located at the downstream exit. Ambient air is drawn into the inlet and through a series of anti-turbulence screens and honeycombs before discharging into the test chamber. The tunnel can provide a free-stream velocity up to 180 ft/s, corresponding to a Mach number of 0.16; a dynamic pressure of 38.5 psf; and a unit Reynolds number of 1.145×10^6 per foot on a standard day. The model support system allows the model attitude to be varied from −10 deg to +90 deg in pitch and −20 deg to +20 deg in yaw. Figure 2 shows the coordinate system of the model.

Model Description

The models used in the experiment were an existing three-percent-scale HXLV model (Fig. 3), and a partial model of the B52-B airplane that was built specifically for this test. The HXLV model was originally built for the Hyper-X program by the addition of an X-43A RV and adapter to an existing Pegasus first stage. The model was machined from stainless steel and represents the outer mold line (OML) of the HXLV configuration with no representation of the thermal protection system (TPS) on the wing and tail surfaces. The added X-43A RV and adapter were cast from stainless steel as one part. As originally built, the three tail surfaces on the model could deflect through a range of −20 deg to +20 deg, in 5-deg increments. For this test, the aft fuselage was modified to allow additional deflections of ±30, ±40, and ±51 deg. The modified fuselage part is shown in Fig. 4. For the HXLV data, the full-scale reference value for moment location is 262 in., the wingspan is 22.0 ft, the wing chord is 8.14 ft, and the wing area is 145.4 ft^2.

The B-52B airplane model was a partial representation of the B-52B carrier airplane, consisting of approximately one-half of the fuselage length and one-third of the starboard wing. No empennage, left wing, or engine pods were included on the model, but the pylon in the starboard wing root was included, along with the cutout in the wing flap for the HXLV vertical tail. The B-52B airplane model was fabricated in sections from a resinous plastic using stereo-lithography technique. Two carbon-fiber rods were added to the wing for stiffness and the partial wing section was bonded into the fuselage. A thin fiberglass skin was added to the outer surface for a smoother surface and to add strength to the model. An aluminum pipe was bonded into the model through the base

and served as a sting support. Figures 5 and 6 show the model installed in the test section of the ViGYAN Low-Speed Wind Tunnel.

The three-percent-scale HXLV model was mounted on a six-component strain-gage balance and attached to the model support system by way of a sting through the base of the model. The balance used for the test was the UT-56 balance. The load ranges of the balance are as follows: normal force = 50 lbf, axial force = 5 lbf, pitching moment = 50 in-lbf, rolling moment = 8 in-lbf, and side force = 10 lbf. The uncertainty of the balance was 0.5-percent full scale. The B-52B airplane model was also mounted to the model support system such that the two models moved in unison through the angle of attack range.

The HXLV was positioned approximately 3/8 in. below the pylon to prevent contact during the wind-tunnel tests (10 in. full scale). The scope of the test precluded actually joining the HXLV to an instrumented pylon. The lower vehicle positioning resulted in approximately 15 percent less downwash effect from the wing of the B-52B airplane. Additionally, this positioning allowed the center portion of the wing of the HXLV to be exposed to the airflow. Both of these effects decreased the influence of the B-52B airplane on the HXLV. In essence, the HXLV was able to produce greater lift (along with other forces and moments) in the lower position than it could when attached to the pylon. Thus, the resulting aerodynamic coefficients were slightly greater in magnitude. Resulting loads from these coefficients yielded a conservative structural safety analysis.

Test Description

The entire one-week test included model setup, calibration, and testing. During the wind tunnel free-stream runs, data were obtained over a limited angle of attack range of either ± 10 deg or ± 2 deg. During all but two of the initial free-stream runs, the angle of sideslip was set to 0 deg.

The test matrix, shown in Table 1, details the 98 data runs that were obtained. The initial 14 runs (not shown) were setup and calibration runs conducted primarily air-off. The corresponding angle of attack polar breakpoints are provided in Table 2. The scope of the test only allowed for relatively coarse breakpoints.

The primary objective for the wind-tunnel test was to obtain aerodynamic data that could be used to calculate the structural pylon loads that result from a worst-case set of HXLV fin deflections. The control surface combinations required for structural analysis are shown in the "Nomenclature" section. The wind-tunnel data were obtained using these specific combinations to include any influences resulting from the combined controls. A more traditional process to obtain the data would have been to deflect each control individually and use superposition to sum the effects. However, superposition assumes the aerodynamics are independent of each other—an assumption that was avoided. The structural analysis was conducted for numerous flight conditions, combinations of inertial loading (maneuvering), and with the addition of gust loads. Thus, data over a large angle of attack range were obtained and used for the structures analysis.

Test Results

Plots of the aerodynamic coefficients, seen in Figs. 7 through 14, show the HXLV baseline data with the controls at zero for both the vehicle in proximity to the B-52B airplane and in free-stream air. The effect of the presence of the B-52B airplane is directly apparent by the increment between the two sets of data. First, the change in slope of the normal-force coefficient, C_N (Fig. 7), with angle of attack shows a 46-percent reduction for the vehicle while under the wing of the B-52B airplane. In effect, this means that the vehicle is not able to generate much normal force at launch until it is free from the proximity of the downwash field of the B-52B airplane. This point is further illustrated in the lift curve shown in Fig. 8. Additional calculations showed that the vehicle does not have sufficient lift at launch to climb. This is a desired effect, making the launch separation analysis easier in that it shows a reduced possibility of re-contact.

The pitching-moment coefficient, C_m (Fig. 9), shows two interesting effects. First, the increment at angle of attack of indicates that the vehicle will tend to pitch down upon launch separation, which is a good trend for no re-contact. Second, the difference in the C_m as compared with the angle of attack slope is a measure of the basic longitudinal static stability. This slope difference represents approximately 20 percent less static margin (less longitudinal stability) when in the presence of the B-52B airplane. The center of gravity for HXLV vehicle 3 was 20 in. further aft than on vehicle 2. On flight 3, the combined effects of an aft center of gravity and the proximity to the

B-52B airplane yielded a vehicle slightly longitudinally unstable at launch and dictated additional separation analysis.

Another parameter of interest was the rolling-moment coefficient, C_l (Fig. 10), caused by the low roll inertia of the HXLV, and the roll-off at launch for previous vehicles. The data show that the vehicle will be induced to roll positive at launch angles of attack below approximately 2 deg. Because of longitudinal stability and an induced roll at launch, the timing to activate the HXLV control system was changed from approximately 0.5 s after launch to approximately 0.2 s for vehicle 3. The vehicle would drop approximately 5 ft before control activation on flight 2, and 2 ft on flight 3.

The yawing-moment coefficient, C_n (Fig. 11), is normally near zero unless the fin is deflected, because the HXLV vertical tail (fin) is located behind the pylon strut. The side-force coefficient, C_Y (Fig. 12), generated shows that there is a significant influence in the presence of the B-52B airplane. Even so, an analysis of the drag coefficient, C_D (Fig. 13), shows that at angles of attack other than near zero there is a decrease in overall drag. Also, axial force, C_A (Fig. 14), follows the same trend as drag, with a decrease in overall axial force with angle of attack other than zero.

A limited evaluation of large control deflections within proximity to the B-52B airplane was also conducted. Data were obtained for HXLV fin deflections of 0, 20, 30, 40, and 51 deg. All data were obtained near zero angle of attack and were for nose-up elevator deflection, nose-left rudder, or right-wing-down aileron. The results showed that the individual fins produced maximum effectiveness at an approximately 30-deg deflection and were effectively stalled by the time the 51-deg mechanical stop was reached. The elevator maximum pitching moment occurred at the 30-deg deflection and was at 65 percent of maximum for 51 deg of elevator deflection. The rudder maximum yawing moment increment occurred at the 30-deg deflection and was 76 percent of maximum at 51 deg of rudder deflection. The aileron incremental rolling moment occurred at 60-deg deflection (total differential elevon angle definition) and was reduced to 84 percent of the maximum value at 102 deg or 51-deg individual deflection of the left and right fin. While the primary control effectiveness decreased beyond 30 deg of fin movement, as expected the drag continued to increase until at 51 deg it was approximately twice the drag at 30 deg.

Separation Model

Prior to flight 3, the wind-tunnel data had only been used for structural analysis studies. The concern of launching flight 3 in a slightly longitudinally statically unstable condition was that the vehicle might be able to pitch and roll enough to strike its vertical tail on the pylon. Thus, a simple launch separation model was developed. The primary data used were the same as those presented in Figs. 7 through 14. The increments in the aerodynamic coefficients between the HXLV in free-stream and in the presence of the B-52B airplane were used to define a set of incremental coefficients that were added to the corresponding total coefficients in a batch simulation. However, these incremental coefficients only define one location 10 in. (0.833 ft) below the pylon. For the simulation, it was necessary to compute a proximity coefficient (*P-factor*) to model how the influence of the wing of the B-52B airplane varied with separation distance. This was accomplished by using a vortex lattice program to calculate the lift slope as a function of distance by using a planar model of the HXLV under a planar model of a B-52B airplane wing (without the pylon). A factor was then derived using the inverse of the increment in the lift curve slope normalized to unity at the 10-in. separation. A factor was calculated at discrete points between 0 and 5 ft below the pylon. Below 5 ft of separation distance, the factor was linearly ramped to zero by the 20-ft point. Justifications for early influence termination were that the HXLV would not hold its longitudinal position directly under the wing of the B-52B airplane (since the B-52B airplane would continue traveling forward as the HXLV would, because of drag, rapidly translate aft) and that the first 5 ft of separation were of primary interest. The resulting proximity *P-factor* is multiplied by each of the incremental aerodynamic coefficients. It is considered conservative, as its starting value is greater than one. In reality, it is likely less than unity when in contact with the pylon. The results of the batch simulation showed the resulting pitch rate increasing to approximately 1 deg/s after launch. This small pitch rate was not a safety concern.

Concluding Remarks

A test was conducted in a low-speed wind tunnel to determine the effectiveness of the Hyper-X launch vehicle fins in the proximity of the B-52B airplane. Test parameters included worst-case scenarios of the fins going to their

hard-over stops of 51 degrees. The results showed that the maximum effectiveness of the surfaces in the influence of the B-52B airplane occurred at approximately 30 degrees at subsonic conditions.

The test obtained aerodynamic coefficients for use in a separation model. The data were obtained in proximity to the B-52B airplane model and then a proximity factor was developed to allow for varying separation distances and their influences to be incorporated in a simulation. The test data were used to formulate a simple launch separation model. The launch separation model was then used to examine the possibility of re-contact, and showed that re-contact was not likely because of the decreased lift capability demonstrated while the model was in the influence of the B-52B airplane.

Testing in the low-speed wind tunnel used the configuration of an existing three-percent-scale Hyper-X launch vehicle model as well as a plastic model of a partial B-52B airplane. These models were used to obtain the aerodynamic influence on load data into the launch pylon. This set of data was then used to perform a conservative structural analysis of the B-52B airplane pylon. The analysis was then used to verify the loads acting on the B-52B airplane pylon and to aid in clearing it for flight.

References

[1]Adolph, C. E., Allavie, J. E., and Bock, Jr., C. C., "Flight Evaluation of the B-52 Carrier Aircraft for the X-15," AFFTC-TR-60-33, September 1960.

[2]Freeman, D., Reubush, D., McClinton, C., Rausch, V., and Crawford, L., "The NASA Hyper-X Program," NASA/TM-97-207243, 1997.

[3]Dominguez, K., Graham, A. B. and DeLoach, R., "Development of an MDOE Compliant Control System in the ViGYAN Low-Speed Wind Tunnel," AIAA-2001-0169, 2001.

Table 1. Test Matrix: X-43A/B-52 hardover fins aerodynamics in the ViGYAN 3-by 4-foot low-speed wind tunnel.

Sequence	Run	Configuration	α	β	de,l, deg	de,r, deg	dr, deg	de, deg	da, deg	Comments
1	16	HXLV freestream	A1	0	0	0	0	0	0	Database comparison check, R
2	15			4	0	0	0	0	0	
3	17			-4	0	0	0	0	0	
4	18			0	10	10	0	10	0	
5	19				-10	10	0	0	20	
6	20				0	0	10	0	0	
7	33,40,(73)	HXLV & B-52	A2	0	0	0	0	0	0	HXLV & B-52, zero controls
8	34,41,46,(76)				0	0	0	0	0	NL
9	35,(74)				0	0	-51	0	0	NR
10	36,39,(50,71)				-51	-51	0	-51	0	NU
11	32, (55,72)				51	51	0	51	0	ND
12	37, (59)				51	-51	0	0	-102	RWD
13	38,62,68				-51	-51	51	-51	0	NL,NU
69	80				-51	51	0	0	102	LWD
14	21,22,23,96,97,98	HXLV freestream	A1	0	0	0	0	0	0	HXLV in freestream flow, R(6)
15	24,30				0	0	51	0	0	R

Run	Point	Vehicle								Notes
16	25				0	0	-51	0	0	
17	26				-51	-51	0	-51	0	
18	27,31				51	51	0	51	0	
19	28				51	-51	0	0	-102	
20					-51	-51	51	-51	0	
65	95				-51	51	0	0	102	
21	42	HXLV & B-52	A3	0	0	0	20	0	0	Aerodynamic trends, rudder
22	43,60				0	0	30	0	0	R
23	44,45				0	0	40	0	0	
24	46				0	0	51	0	0	
25	47				-20	-20	0	-20	0	
26	48				-30	-30	0	-30	0	
27	49				-40	-40	0	-40	0	
28	50				-51	-51	0	-51	0	
29	52				20	20	0	20	0	Aerodynamic trends negative elevon
30	53,61				30	30	0	30	0	R
31	54				40	40	0	40	0	
32	55				51	51	0	51	0	
33	56				20	-20	0	0	-40	Aerodynamic trends, aileron
34	57				30	-30	0	0	-60	
35	58				40	-40	0	0	-80	
36	59				51	51	0	0	-102	
38	63	HXLV & B-52	A2	0	-51	-51	-51	-51	0	NR,NU
37	38,62,68				-51	-51	51	-51	0	NL,NU (repeat sequence 13)
40	64,69				51	51	-51	51	0	NR,ND
39	65				51	51	51	51	0	NL,ND
41	78				-51	51	-51	0	102	NR, LWD
42	79				51	-51	51	0	102	NR, LWD
51	66				-51	51	51	0	102	NL, LWD
52	67				51	-51	-51	0	-102	NR,RWD
43	70	HXLV & B-52	-5	0	0	0	0	0	0	MDOE, Block 2
44	71		0	0	-51	-51	0	-51	0	
45	72		0	0	51	51	0	51	0	
46	73		0	0	0	0	0	0	0	
47	74		0	0	0	0	-51	0	0	
48	75		5	0	0	0	0	0	0	
49	76		0	0	0	0	51	0	0	
50	77		0	0	0	0	0	0	0	
53	83	HXLV & B-52	0	0	0	0	0	0	0	MDOE, Block 1
54	84		3	0	-30	-30	-30	-30	0	
55	85		30	0	30	30	30	30	0	
56	86		0	0	0	0	0	0	0	
57	87		-3	0	-30	-30	-30	-30	0	
58	88		0	0	0	0	0	0	0	
59	89		-3	0	30	30	30	30	0	
60	90		-3	0	30	30	-30	-30	0	
61	91		3	0	-30	-30	30	-30	0	

62	92	0	0	0	0	0	0	0
63	93	-3	0	-30	-30	30	-30	0
64	94	3	0	30	30	-30	30	0

Table 2. Angle of attack polars.

Angle of attack polar	Points
A1	-10,-8,-6,-4,-2,0,2,4,6,8,10,12,14,16 deg
A2	-10,-5,0,5,10 deg
A3	-2,-1,0,1,2 deg

Figures

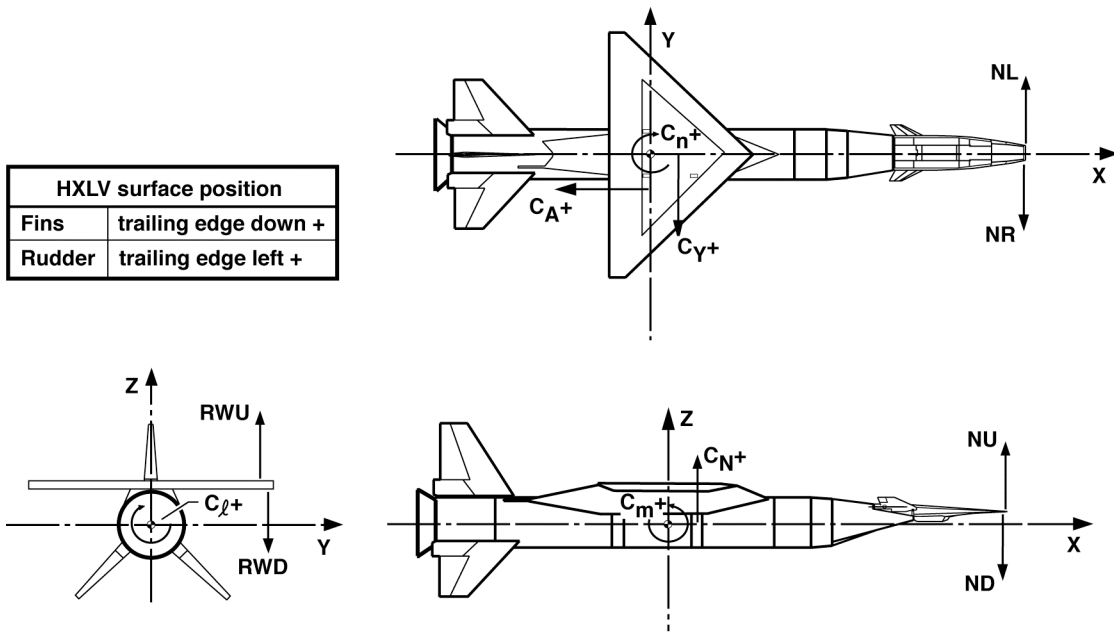Figure 1. The B-52B airplane carrying the Hyper-X launch vehicle stack.

American Institute of Aeronautics and Astronautics

Figure 2. The coordinate system of the three-percent-scale Hyper-X launch vehicle stack model.
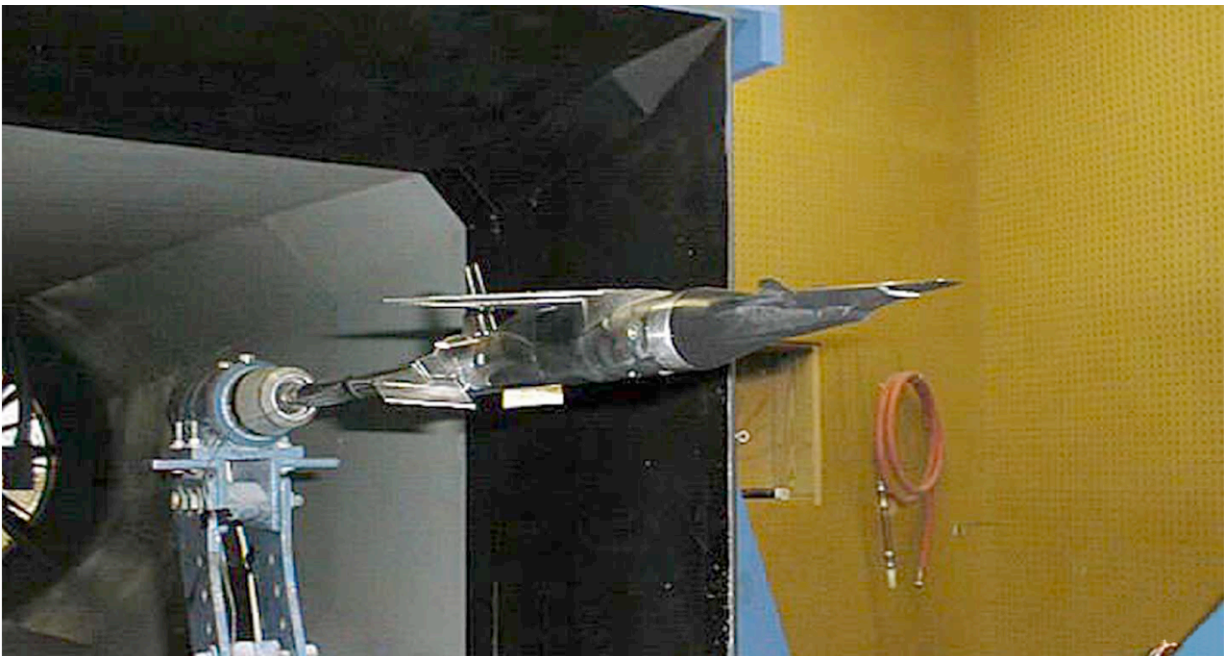
Figure 3. The three-percent-scale Hyper-X launch vehicle stack model in the ViGYAN 3- by 4-foot Low-Speed Wind Tunnel.

American Institute of Aeronautics and Astronautics

Figure 4. The modified tail-can of the three-percent-scale Hyper-X launch vehicle stack model with fin settings of 51 degrees.
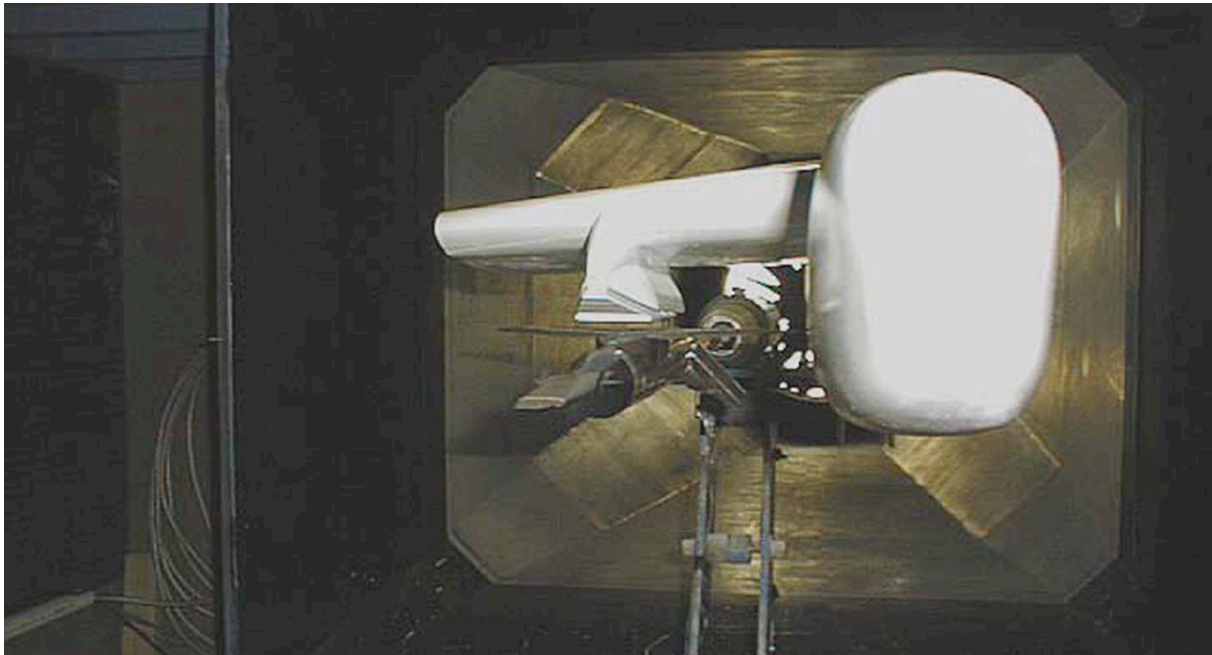
Figure 5. Front view of the partial B-52B airplane model with the three-percent-scale Hyper-X launch vehicle stack model.

Figure 6. Side view of the partial B-52B airplane model with the three-percent-scale Hyper-X launch vehicle stack model.
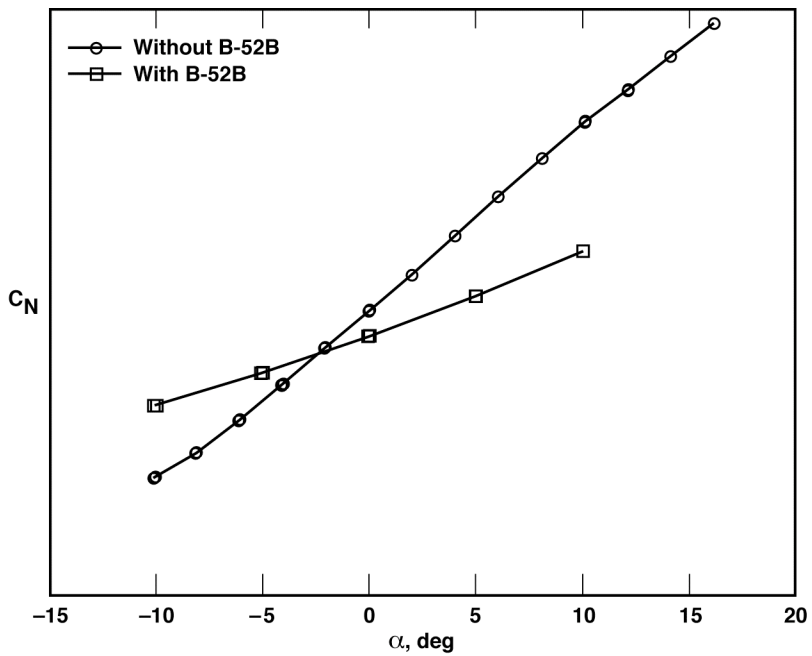
Figure 7. The Hyper-X launch vehicle normal-force coefficient with and without the influence of the partial B-52B airplane model.
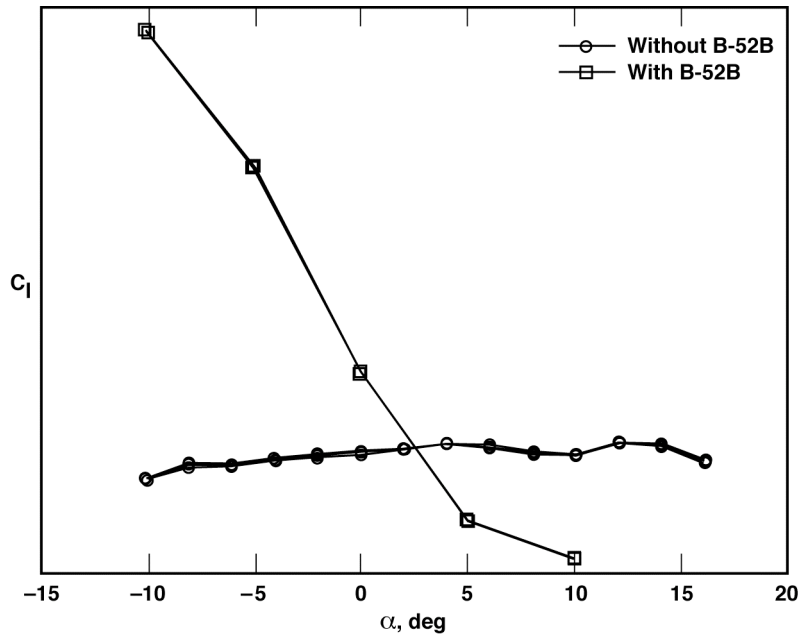
American Institute of Aeronautics and Astronautics
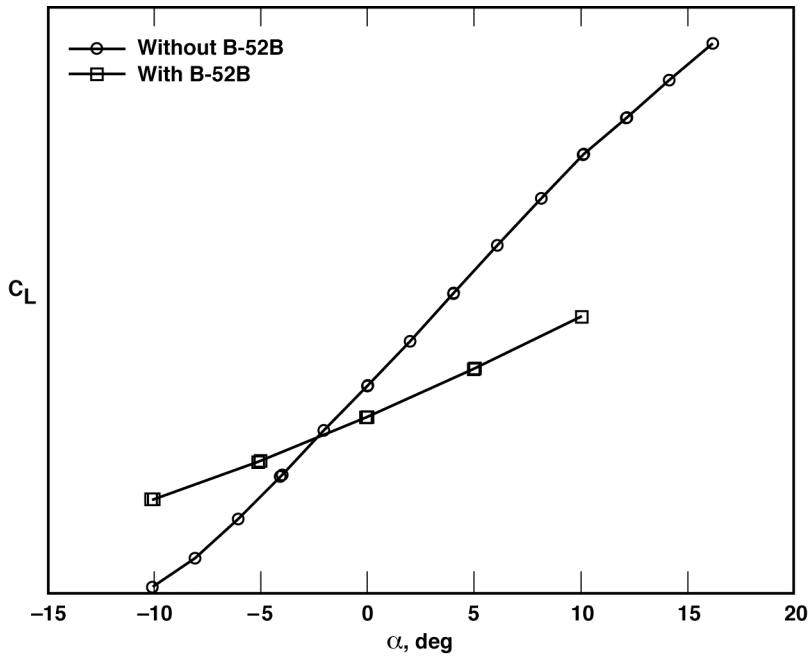
Figure 8. The Hyper-X launch vehicle lift coefficient with and without the influence of the partial B-52B airplane model.
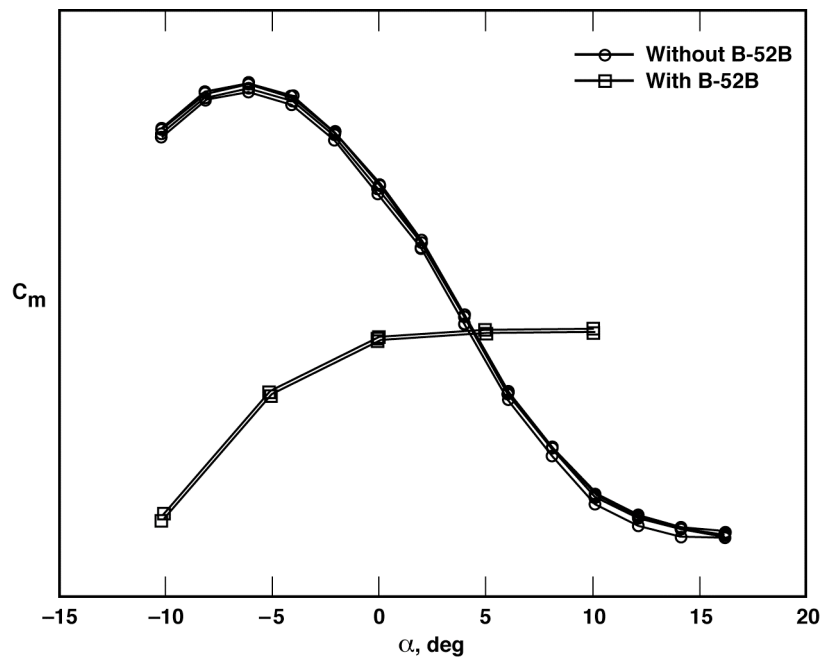
Figure 9. The Hyper-X launch vehicle pitching-moment coefficient with and without the influence of the partial B-52B airplane model.

Figure 10. The Hyper-X launch vehicle rolling-moment coefficient with and without the influence of the partial B-52B airplane model.
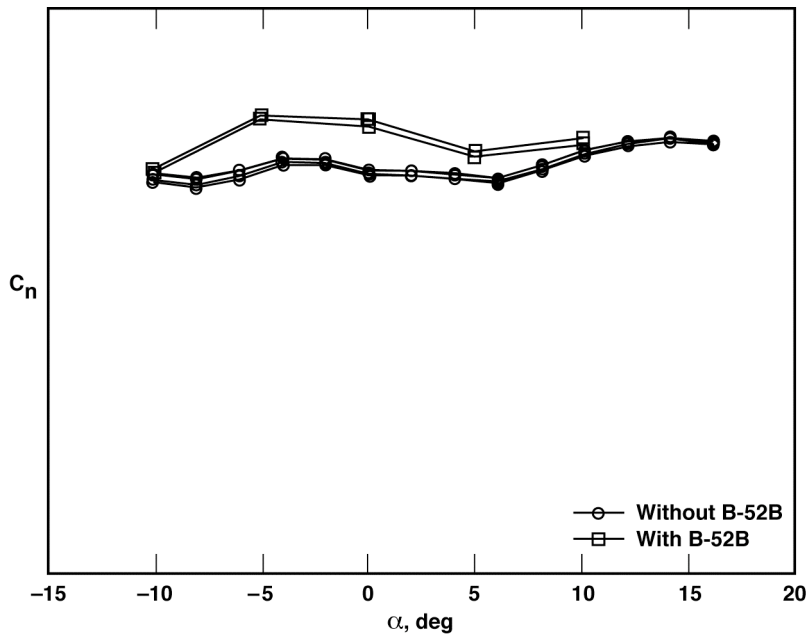

Figure 11. The Hyper-X launch vehicle yawing-moment coefficient with and without the influence of the partial B-52B airplane model.
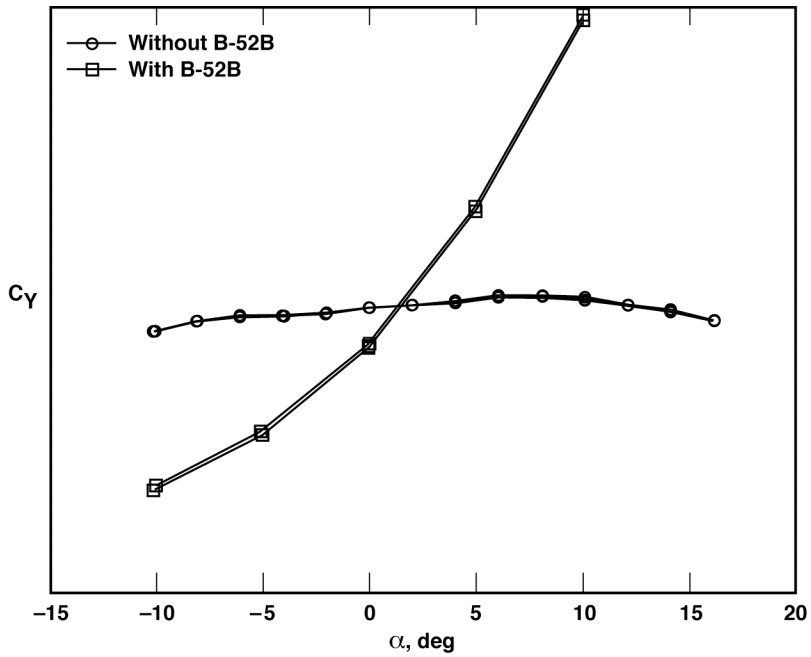
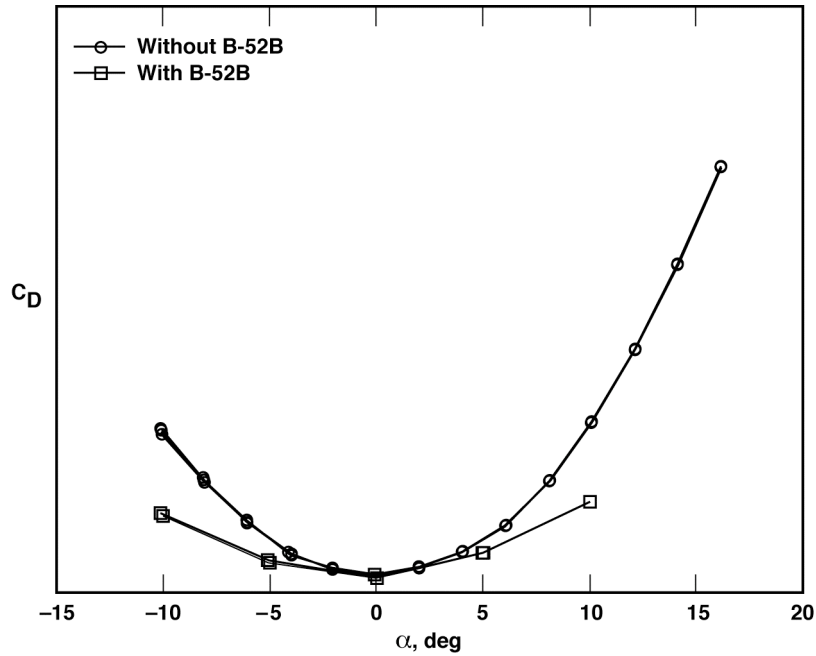American Institute of Aeronautics and Astronautics

Figure 12. The Hyper-X launch vehicle side-force coefficient with and without the influence of the partial B-52B airplane model.

Figure 13. The Hyper-X launch vehicle drag coefficient with and without the influence of the partial B-52B airplane model.

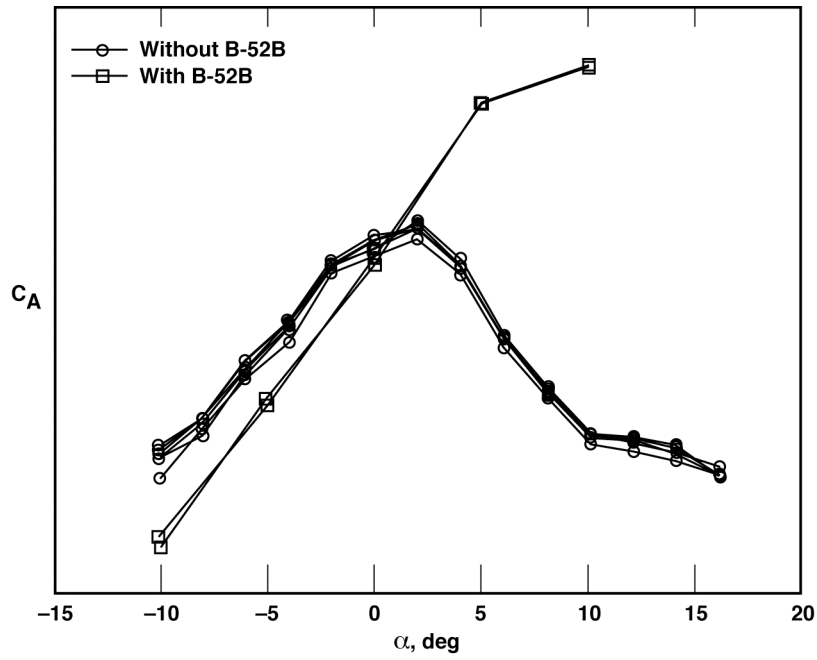American Institute of Aeronautics and Astronautics

Figure 14. The Hyper-X launch vehicle axial-force coefficient with and without the influence of the partial B-52B airplane model.

American Institute of Aeronautics and Astronautics